Title

Fat Composition Changes in Bone Marrow During Chemotherapy and Radiation Therapy

Journal

International Journal of Radiation Oncology • Biology • Physics, 90(1)

ISSN

0360-3016

Authors

Carmona, Ruben
Pritz, Jakub
Bydder, Mark
et al.

Publication Date

2014-09-01

DOI

10.1016/j.ijrobp.2014.05.041

Peer reviewed

International Journal of Radiation Oncology biology • physics

www.redjournal.org

Clinical Investigation

Fat Composition Changes in Bone Marrow During Chemotherapy and Radiation Therapy

Ruben Carmona, MD, MAS,* Jakub Pritz, PhD,* Mark Bydder, PhD,† Sachin Gulaya, BS,* He Zhu, MD, PhD,* Casey W. Williamson, BA,* Christian S. Welch, MD,† Florin Vaida, PhD,‡ Graeme Bydder, MD,† and Loren K. Mell, MD*

**Department of Radiation Medicine and Applied Sciences, University of California San Diego, La Jolla, California; †Department of Radiology, University of California San Diego Medical Center, San Diego, California; and ‡Biostatistics and Bioinformatics, Department of Family and Preventive Medicine, University of California San Diego Medical Center, San Diego, California*

Received Mar 27, 2014, and in revised form May 12, 2014. Accepted for publication May 19, 2014.

Summary

Magnetic resonance imaging fat quantification is sensitive to vertebrae bone marrow composition changes that result from chemoradiation therapy. These findings indicate that locoregional effects of chemoradiation likely contribute to the clinical manifestation of myelosuppression.

Purpose: To quantify changes in bone marrow fat fraction and determine associations with peripheral blood cell counts.

Methods and Materials: In this prospective study, 19 patients received either highly myelotoxic treatment (radiation therapy plus cisplatin, 5-fluorouracil mitomycin C [FU/MMC], or cisplatin/5-FU/cetuximab) or less myelotoxic treatment (capecitabine-radiation therapy or no concurrent chemotherapy). Patients underwent MR imaging and venipuncture at baseline, midtreatment, and posttreatment visits. We performed mixed effects modeling of the mean proton density fat fraction (PDFF[%]) by linear time, treatment, and vertebral column region (lumbar [L] 4-sacral [S]2 vs thoracic [T]10-L3 vs cervical[C]3-T9), while controlling for cumulative mean dose and other confounders. Spearman rank correlations were performed by white blood cell (WBC) counts versus the differences in PDFF(%) before and after treatment.

Results: Cumulative mean dose was associated with a 0.43% per Gy ($P=.004$) increase in PDFF(%). In the highly myelotoxic group, we observed significant changes in PDFF(%) per visit within L4-S2 (10.1%, $P<.001$) and within T10-L3 (3.93%, $P=.01$), relative to the reference C3-T9. In the less myelotoxic group, we did not observe significant changes in PDFF(%) per visit according to region. Within L4-S2, we observed a significant difference between treatment groups in the change in PDFF(%) per visit (5.36%, $P=.04$). Rank correlations of the inverse log differences in WBC versus the differences in PDFF(%) overall and within T10-S2 ranged from 0.69 to 0.78 ($P<.05$). Rank correlations of the inverse log differences in absolute

Reprint requests to: Loren K. Mell, MD, Department of Radiation Medicine and Applied Sciences, 3855 Health Sciences Dr, MC0843 La Jolla, CA 92093. Tel: (858) 246-0471; E-mail: lmell@ucsd.edu

This research was funded by National Cancer Institute grant 1R21CA162718-01 and GE Healthcare. The sponsors had no role in the preparation of this manuscript.

Int J Radiation Oncol Biol Phys, Vol. 90, No. 1, pp. 155–163, 2014
0360-3016/$ - see front matter Published by Elsevier Inc.
http://dx.doi.org/10.1016/j.ijrobp.2014.05.041

neutrophil counts versus the differences in PDFF(%) overall and within L4-S2 ranged from 0.79 to 0.81 ($P<.05$).

Conclusions: Magnetic resonance imaging fat quantification is sensitive to marrow composition changes that result from chemoradiation therapy. These changes are associated with peripheral blood cell counts. This study supports a rationale for bone marrow-sparing treatment planning to reduce the risk of hematologic toxicity. Published by Elsevier Inc.

Introduction

A limiting factor in cancer treatment with chemoradiation therapy is marrow toxicity (1, 2). Bone marrow is composed of red and yellow marrow. Red marrow consists of hematopoietic stem cells that produce erythrocytes, leukocytes, and thrombocytes. Yellow marrow, like red marrow, contains abundant capillaries but is not directly involved in hematopoiesis. The stroma of the reticular network of yellow marrow is filled primarily with lipids, thus exhibiting a higher fat content. Red marrow is found in flat bones including the pelvis, sternum, and vertebrae, whereas yellow marrow is found in the medullary cavities of long bones. Both chemotherapy and radiation suppress the hematopoietic system, leading to a reduction in red marrow and an increase in yellow marrow (3). This composition change can result in neutropenia and thrombocytopenia that require chemotherapy dose reductions and delays, thus compromising treatment outcomes (4, 5).

T1-weighted magnetic resonance imaging (MRI) provides a qualitative impression of the amount of fat present in bone marrow due to the short T1 of fat compared to that in other tissues. Although this approach is sufficient for distinguishing low-fat from high-fat content, T1-weighting is not reliable when quantitative results and/or finer distinctions are required. A quantitative measure of bone marrow fat fraction is the iterative decomposition of water and fat with echo asymmetrical and least squares estimation (IDEAL) imaging technique, which can be used to create parametric fat fraction maps, providing both quantitative and spatially resolved information on marrow composition (6-10). Liang et al (11) showed that fat fraction maps have sufficient spatial resolution to be used in radiation therapy (RT) planning in patients undergoing pelvic chemoradiation.

Bolan et al (12) showed that water-fat MRI could be used to assess changes in bone marrow fat content in patients with gynecologic malignancies pre- and postchemotherapy and RT. These investigators showed that chemotherapy-induced changes are uniform in space and that radiation-induced changes are consistent with red-to-yellow marrow transformation. Although they showed an increase in marrow fat fraction at the lumbar (L)4 level from baseline to 6 months posttreatment they did not provide quantitative data for other vertebrae. Furthermore, they did not test differences in the magnitude, rate, and pattern of change between treatment groups or how fat fraction changes related to clinically significant variables such as the development of neutropenia.

The primary aim of this study was to assess the magnitude, rate, and pattern of change in vertebrae bone marrow fat fraction for patients receiving highly myelotoxic versus less myelotoxic pelvic chemoradiation therapy and versus RT alone. The study's secondary aim was to determine associations between peripheral blood cell counts and fat fraction changes. Measuring composition changes over the course of treatment may provide quantitative spatial evidence to support bone marrow-sparing treatment planning approaches.

Methods and Materials

Study design and patients

This prospective, longitudinal, single-site clinical study was approved by the institutional review board and is compliant with the Health Insurance Portability and Accountability Act. The population consisted of patients undergoing pelvic chemoradiation therapy or RT alone for gynecologic, anorectal, or genitourinary malignancies. Subjects treated with palliative intent were excluded. Subjects were recruited from the institution's radiation oncology clinics. All subjects provided informed consent. Our research budget afforded screening of 27 subjects, from November 2008 to July 2012, with 19 patients electing to participate (9 cervical cancer, 2 endometrial cancer, 3 anal cancer, 1 rectal cancer, and 4 prostate cancer patients).

Treatment

All patients received intensity modulated RT (IMRT). Four prostate cancer patients received pelvic RT only, 45.0 Gy in 1.8-Gy fractions to the pelvis, followed by a sequential boost to a total dose of 75.6 to 81.0 Gy. Two endometrial cancer patients underwent hysterectomy followed by adjuvant therapy with carboplatin (area under the curve = 6) and paclitaxel (175 mg/m^2, intravenously [IV]) for 6 cycles, followed by pelvic RT, 45.0 to 50.4 Gy in 1.8-Gy fractions. Anal cancer patients received 45 to 58.2 Gy in 1.5- to 2.0-Gy fractions with either concurrent 5-fluorouracil (5-FU; 1000 mg/m^2 IV, on days 1-4 and 29-32) and mitomycin-C (MMC; 10 mg/m^2 IV, on days 1 and 29; 2 patients) or cisplatin (75 mg/m^2 IV every 28 days × 2), 5-FU

(1000 mg/m^2 IV on days 1-4 every 28 days × 2), and cetuximab (400 mg/m^2 loading dose and then 250 mg/m^2/week, IV, every 6-8 weeks; 1 patient). Nine cervical cancer patients received pelvic RT, 45.0 to 50.4 Gy in 1.8-Gy fractions, with concurrent cisplatin, 40 mg/m^2 weekly, followed by high-dose rate brachytherapy (30 Gy in 5 fractions to point A). One rectal cancer patient received pelvic RT, 50.4 Gy in 1.8-Gy fractions, with concurrent capecitabine therapy (825 mg/m^2, twice daily for 5 days per week). One of 3 anal cancer patients and 1 of 2 uterine cancer patients received pelvic-inguinal radiation. Two of 9 cervical cancer patients received extended field (ie, pelvic-para-aortic) RT. All patients completed chemoradiation therapy without treatment delays, and no patients received granulocyte colony-stimulating factors.

For this study, we broadly classified treatment into 2 main categories: highly myelotoxic treatment and less myelotoxic treatment (Table 1). The highly myelotoxic treatment group consisted of cervical cancer patients treated with cisplatin and anal cancer patients treated with 5-FU/MMC or cisplatin/5-FU/cetuximab. The less myelotoxic treatment group consisted of patients who received no concurrent chemotherapy or concurrent capecitabine.

Concurrent imaging and laboratory blood tests

Patients underwent MRI with quantitative IDEAL (IDEAL-IQ) at baseline (within a 30-day window), midtreatment (within a 14-day window), and posttreatment (within 30 days of completion). MRI scans were performed with a 3.0-T scanner (Signal HDx; GE Healthcare, Milwaukee, WI). A spinal phased array coil was used. The IDEAL-IQ sequence is a multiple echo 3-dimensional (3D) spoiled gradient echo with a typical TR of 10 ms; a flip angle of 3°; and 6 echo times of between 1.0 and 6.0 ms. The technique estimates fat fraction and R^2 with corrections included for B0 inhomogeneity, fat spectrum, and noise bias. Sagittal spinal scans were obtained with each study. White blood cell counts (WBC) and absolute neutrophil counts (ANC) were collected at baseline and weekly thereafter for patients undergoing chemoradiation therapy. Prostate cancer patients did not undergo serial blood count measurements. Peripheral blood counts obtained closest to the time of each MRI acquisition (within a 7-day window) were used for the analysis.

Image analysis and dose calculation

A 2D region of interest (ROI) was drawn at the center of each subject's vertebrae (cervical [C]3 to sacral [S]2) from serial sagittal spine MRIs, using the Digital Images and Communication in Medicine (DICOM) viewer (version 4.1; Osirix; Osirix Foundation, Geneva, Switzerland) (13). Each ROI contained approximately 100 to 200 voxels. The vertebral ROIs were positioned to include vertebral body bone marrow and to avoid areas of partial volume and

Table 1 Patient, tumor and treatment characteristics

Characteristic	Highly myelotoxic	Less myelotoxic	All	*P*
No. of patients	12	7	19	
Mean age (±SD), yrs	48 (±13)	62 (±7)	53 (±13)	.006
No. of women (%)	10 (83%)	3 (43%)	13	.17
Racial distribution, n (%)				.34
Caucasian	7 (58%)	6 (86%)	13	
Hispanic	4 (33%)	0 (0%)	4	
Asian	1 (8%)	1 (14%)	2	
Mean body mass index (±SD), kg/m^2	26.2 (±6)	26.3 (±6.1)	26.2 (±5.8)	.99
Cancer site: stage (n)	Cervix: IBI (4), IB2 (2) IIB2 (2), IIIB (1) Anus: IIIA (3)	Uterus: IIIB (1), IV (1) Rectum: IIIA (1) Prostate: III (4)	Cervix (9); Uterus (2) Anus: 3; Rectum: 1 Prostate: 4	
Chemotherapy (n)	CDDP (9) 5-FU/MMC (2) CDDP/5-FU/cetuximab (1)	CAP (1) No concurrent chemo (6)	CDDP (9); 5-FU/MMC (2) CDDP/5-FU/cetuximab (1) CAP (1) No concurrent chemotherapy (6)	
No. undergoing pretreatment chemotherapy (%)	0 (0%)	3 (43%)	3	.04
No. undergoing IMRT (%)	12 (100%)	7 (100%)	19	1.0
No. undergoing pelvic-aortic RT (%)	2 (17%)	0 (0%)	2	.51
No. undergoing pelvic-inguinal RT (%)	1 (8%)	1 (14%)	2	1.0
Mean WBC × 10^3/μ (±SD)	7.25 (±2.5)	6.3 (±0.5)	16	.58
Mean ANC × 10^3/μ (±SD)	4.6 (±1.9)	3.7 (±0.4)	14	.22

Abbreviations: 5-FU = 5-fluorouracil; ANC = absolute neutrophil count; CAP = capecitabine; CDDP = cisplatin; IMRT = intensity modulated radiation therapy; MMC = mitomycin C; RT = radiation therapy; SD = standard deviation; WBC = white blood cell count.

image artifact. Each ROI was inspected and manually adjusted if necessary to account for subject motion between scans. The mean signal intensity within the ROI provided corresponding vertebrae marrow proton density fat fraction (PDFF) values. PDFF in a given sample is defined as the number of protons in fat (triglycerides) divided by the total number of protons (water plus fat) expressed as percentages (PDFF[%]) from 0 to 100 (6). ROIs were grouped into 3 vertebral column regions: lumbar (L)4 to S2 (the area consistently receiving large doses within the pelvic field), thoracic (T)10 to L3 (the area superior to the pelvic field receiving variable doses), and C3 to T9 (area receiving no dose). Grand mean PDFF(%) values were calculated for each subject according to region. From the radiation treatment plans, cumulative mean doses (Gy) were calculated for each subject according to region at mid- and posttreatment visits.

Statistical analysis

Student's *t*, Mann-Whitney *U*, and Fisher's exact tests were used to analyze baseline differences in age, race, sex, body mass index (BMI), WBC, and ANC between the highly myelotoxic and less myelotoxic treatment groups. To estimate the effects of myelotoxic chemotherapy on fat fraction, we performed linear mixed effects (LME) modeling of the mean PDFF(%), with fixed interaction and main effects terms for chemotherapy (highly myelotoxic vs less myelotoxic), cumulative mean dose (continuous, Gy), time (continuous), and location within the vertebral spine (L4-S2 vs T10-L3 vs C3-T9) (14, 15). Akaike's information criterion (AIC) Muller S, Scealy JL, Welsh AH. Model Selection in Linear Mixed Models. Statistical Science 2013; 28:135-167. Based on the maximum likelihood (ML) was used to select the linear-time model versus a profile-time model. Model parameter estimation was based on restricted maximum likelihood (16). To control for correlated observations within subjects, we created a subject-specific random slope for time and included it in the LME model. We tested the effects of potential confounders: age (continuous, mean centered) and whether subjects received pretreatment chemotherapy (yes vs no). Due to the risk of model overfitting, we did not test the effects of other potential confounders, such as BMI. All possible secondary and tertiary interaction terms were tested. Forward and backward elimination were performed, and main effects and interaction terms were significant at *P* values of $\leq$.20 and $\leq$.05, respectively.

To test associations between peripheral blood cell counts and bone marrow fat fraction, we performed Spearman rank correlations for the differences in mean proton density fat fraction (ΔPDFF[%]) between the end of treatment (t_2) and baseline (t_0) versus $-\log(WBC_{t2}/WBC_{t0})$, $-\log(ANC_{t2}/ANC_{t0})$, and WBC and ANC nadirs (lowest values occurring during RT). Rank correlation statistics were computed overall and according to vertebral column region. All tests were two-tailed, with significant correlations at a *P* value of $\leq$.05. Data were prepared and analyzed using R version 2.15.1 software (http://www.r-project.org).

Results

Twelve patients received highly myelotoxic treatment and 7 patients received less myelotoxic treatment (Table 1). The median age was 55 years of age (range: 27-81 years). Patients were younger in the highly myelotoxic treatment group. There were no differences in race, BMI, WBC, and ANC between treatment groups.

Fifteen of 19 patients completed all 3 IDEAL-IQ scans (baseline, midtreatment, and posttreatment Two patients completed only the baseline and midtreatment scans, 1 patient completed only the baseline and posttreatment scans, and 1 patient completed only the midtreatment and posttreatment scans. Altogether, 18, 18, and 17 patients completed the baseline, midtreatment, and posttreatment scans, respectively. The mean ($\pm$SD) number of days from the baseline IDEAL-IQ scan to the midtreatment and post-treatment scans were 24 ($\pm$10) and 55 ($\pm$13) days, respectively.

Twelve patients completed all 3 WBC draws (baseline, midtreatment, and posttreatment). Two patients completed only the baseline and midtreatment WBC draws, 1 patient completed only the baseline and posttreatment WBC draws, and 1 patient completed only the baseline WBC draw. Altogether, 16, 14, and 13 patients completed the baseline, midtreatment, and posttreatment WBC measurements, respectively. The mean ($\pm$SD) number of days for the WBC measurements relative to the baseline, midtreatment, and posttreatment MRI scans were 2 ($\pm$5), $-$1 ($\pm$3), and 1 ($\pm$6) days, respectively.

Nine patients completed all 3 ANC draws (baseline, midtreatment, and posttreatment). Two patients completed only the baseline and midtreatment ANC draws, 1 patient completed only the baseline and posttreatment ANC draws, 1 patient completed only the midtreatment and posttreatment ANC draws, and 1 patient completed only the baseline ANC test. Altogether, 14, 12, and 11 patients completed the baseline, midtreatment, and posttreatment WBC measurements, respectively. The mean ($\pm$SD) number of days for the WBC measurements relative to the baseline, midtreatment, and posttreatment MRI scans were 1 ($\pm$5), $-$1 ($\pm$3), and 1 ($\pm$6) days, respectively.

Mean PDFF(%) values and cumulative mean doses are shown in Table 2. At baseline, mean PDFF(%) was significantly lower in the highly myelotoxic treatment group than in the less myelotoxic treatment group (37.5% vs 53.6%, respectively, $P<.001$), likely due to the fact that some patients in the low myelotoxic group received pretreatment chemotherapy. Figure 1 shows a representative image of a subject who received highly myelotoxic chemoradiation therapy (Fig. 1 A-C) compared to a subject who received RT alone (Fig. 1 D-F). Images were produced at baseline, at midtreatment, and upon completion of

Table 2 Mean PDFF(%) and cumulative mean dose by MRI study visit, treatment group, and vertebral column region

		Baseline		Midtreatment		Posttreatment	
Treatment group	Region	PDFF(%)	Cumulative dose (Gy)	PDFF(%)	Cumulative dose (Gy)	PDFF(%)	Cumulative dose (Gy)
Highly myelotoxic	C3-T9	33.0 (11.1)	0	34.9 (11.5)	0	30.5 (15.5)	0
	T10-L3	36.0 (13.9)	0	41.2 (14.1)	0.42 (0.78)	42.0 (18.7)	0.60 (1.07)
	L4-S2	43.2 (16.5)	0	64.3 (15.5)	19.3 (5.85)	74.1 (15.5)	28.3 (5.37)
	All vertebrae (C3-S2)	37.5 (14.4)	0	46.5 (18.3)	6.77 (9.79)	49.7 (23.7)	9.93 (13.9)
Less myelotoxic	C3-T9	47.2 (11.5)	0	48.0 (11.0)	0	41.4 (11.3)	0
	T10-L3	52.6 (12.8)	0	51.8 (13.4)	0.17 (0.11)	47.9 (11.7)	0.28 (0.09)
	L4-S2	61.6 (11.2)	0	70.3 (14.2)	18.9 (7.68)	77.8 (12.7)	28.0 (3.86)
	All vertebrae (C3-S2)	53.6 (13.1)	0	57.1 (15.3)	6.67 (10.2)	55.8 (18.9)	9.41 (13.7)

Abbreviations: C = cervical vertebrae; L = lumbar vertebrae; PDFF(%) = proton density fat fraction; S = sacral vertebrae; T = thoracic vertebrae.

treatment. Qualitatively, patients in Figure 1 A-C appear to have higher increases in fat fraction during treatment than those in Figure 1 D-F. To help readers differentiate among signal intensities, we show PDFF(%) values for L5 ROI's: for the subject receiving highly myelotoxic treatment, L5 progressively increases during treatment (59.4%-78.5%-92.1%, respectively), and for the subject receiving only RT, L5 slightly increases but then decreases at the end treatment (59.5%-65.8%-63.8%, respectively).

Figure 2 shows mean differences in PDFF(%) for regions T10-L3 (Fig. 2A) and L4-S2 (Fig. 2B) relative to the reference (C3-T9) by group and visit. At baseline, the relative differences in PDFF(%) for both regions are higher for the less myelotoxic group. However, over the course of treatment, we observed greater differences in PDFF(%) within both regions in the highly myelotoxic group compared to the less myelotoxic group.

Table 3 shows adjusted mean PDFF(%) estimates by MRI study visit, treatment group, vertebral column region, and confounders, with less myelotoxic treatment than the reference group. In the less myelotoxic group, we observed significant increases at baseline in mean PDFF(%) within T10-L3 and L4-S2 relative to that in C3-T9 (intercept). When we performed the analysis with highly myelotoxic treatment as the reference group (as opposed to less myelotoxic treatment shown in Table 3), we also observed

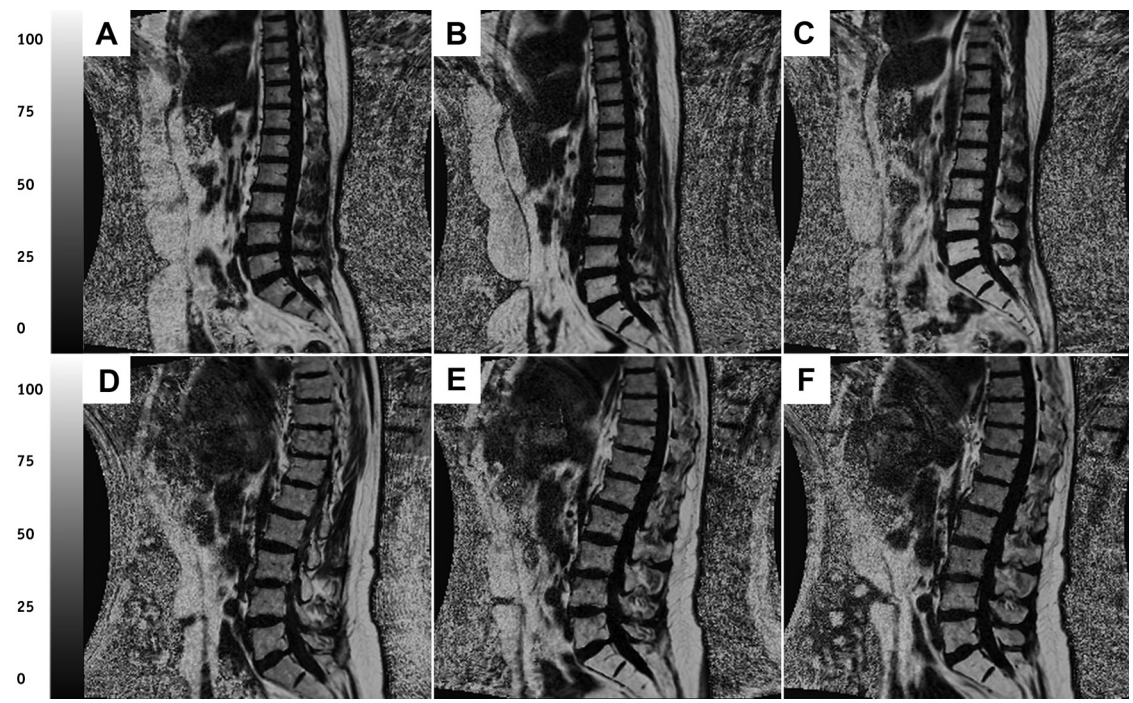

Fig. 1. (A-C) MRIs from a subject with cervical cancer who received cisplatin chemotherapy and IMRT. (D-F) MRIs from a subject with prostate cancer who received IMRT alone. (A and D) Baseline results; (B and E) midtreatment; (C and F) immediately after treatment. PDFF(%) values for L5 regions of interest are (A) 59.4%, (B) 78.5%, (C) 92.1%, (D) 59.5%, (E) 65.8%, and (F) 63.8%. IMRT = intensity modulated radiation therapy; MRI = magnetic resonance imaging; PDFF = proton density fat fraction.

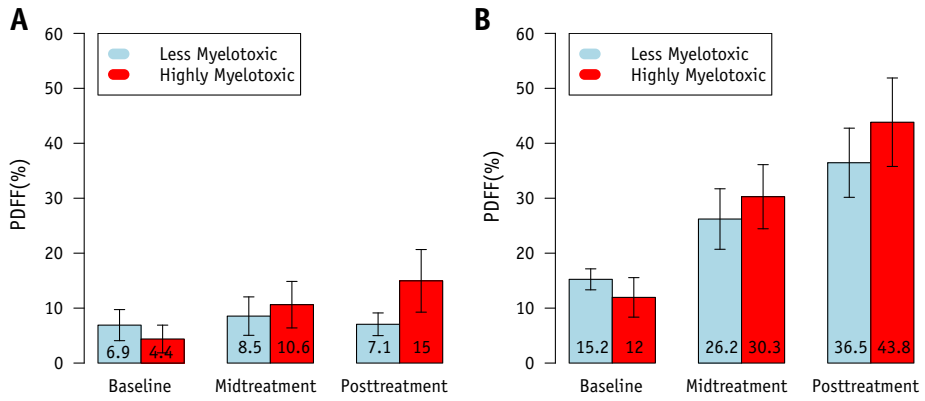

Fig. 2. Bar plots of the mean difference (95% CI) in proton density fat fraction (PDFF[%]) for (A) T10-L3 and (B) L4-S2 relative to C3-T9 by treatment group and visit. PDFF(%) values are labeled within the bars. PDFF = proton density fat fraction.

significant increases at baseline in mean PDFF(%) within T10-L3 (4.48%, 95% confidence interval [CI]: 0.63%-8.32%, $P=.02$) and L4-S2 (11.6%, 95% CI: 7.73%-5.5%, $P<.001$) relative to that in C3-T9 (34.5%, 95% CI: 2.78%-1.2%, $P<.001$). The adjusted model with less myelotoxic treatment as the reference (Table 2) showed no significant differences between treatment groups for each region at baseline. Similarly, we observed no differences when we excluded patients who received pretreatment chemotherapy. Pretreatment chemotherapy was associated with an increase in baseline PDFF(%) of 12.8% (95% CI: −2.70% to 28.2%), and age was associated with an increase in PDFF(%) of 0.39% per year (95% CI: 5.6e-4% to 0.79%). We observed a significant effect of cumulative mean dose on the mean PDFF(%) (0.43% per Gy, 95% CI: 0.13%-0.72%). In the less myelotoxic group, we observed no significant differences among the changes in mean PDFF(%) per visit according to region. With highly myelotoxic treatment as the reference group, we observed significant differences in the changes in mean PDFF(%) per visit according to T10-L3 (3.93% per visit, 95% CI: 0.90-6.96, $P=.01$) and L4-S2 (10.1% per visit, 95% CI: 5.01-15.2, $P<.001$) relative to that of C3-T9. These effects were still present when we excluded patients who received extended field RT (T10-L3: 3.44% per visit, 95% CI: 0.12%-6.77%, $P=.04$; L4-S2: 9.06% per visit, 95% CI: 2.50%-15.6%, $P=.006$). For the highly myelotoxic group relative to the less myelotoxic group, we observed significant differences in changes in PDFF(%) per visit within L4-S2 (5.36% per visit, 95% CI: 0.29%-10.4%). We

Table 3 Adjusted mean PDFF(%) estimates and 95% CI by MRI study visit, treatment group, vertebral column region and confounders

	Parameter	Mean PDFF(%)	*P*
Baseline estimates for the less myelotoxic group	C3-T9 (intercept)	37.3 (25.7-49.0)	<.001
	T10-L3	+5.94 (0.71-11.2)	.02
	L4-S2	+13.9 (8.68-19.2)	<.001
Difference in estimates for the highly myelotoxic group relative to the less myelotoxic group at baseline	C3-T9	−2.83 (−18.2 to 12.5)	.70*
	T10-L3	−1.45 (−7.95 to 5.03)	.66*
	L4-S2	−2.33 (−8.82 to 4.16)	.48*
Change in PDFF(%) per visit for the less myelotoxic group	C3-T9	+1.84 (−6.03 to 2.34)	.38
	T10-L3	+0.37 (−3.69 to 4.44)	.86
	L4-S2	+4.76 (−1.00 to 10.5)	.10
Difference in the change in PDFF(%) per visit between the highly myelotoxic and less myelotoxic groups	C3-T9	+1.50 (−3.74 to 6.73)	.57†
	T10-L3	+3.56 (−1.51 to 8.63)	.16†
	L4-S2	+5.36 (0.29-10.4)	.04†
	Cumulative dose (per Gy)	+0.43 (0.13-0.72)	.004
	Pretreatment chemotherapy	+12.8 (−2.70 to 28.2)	.08
	Age (per yr)	+0.39 (5.6e-4 to 0.79)	.05

Abbreviations: C = cervical vertebra; L = lumbar vertebra; PDFF(%) = proton density fat fraction (%); S = sacral vertebrae; T = thoracic vertebra.

* *P* value is testing differences in mean PDFF(%) for the highly myelotoxic group relative to that of the less myelotoxic group at baseline by vertebral column region.

† *P* value is testing differences in the change in mean PDFF(%) per visit for the highly myelotoxic group relative to that of the less myelotoxic group by vertebral column region.

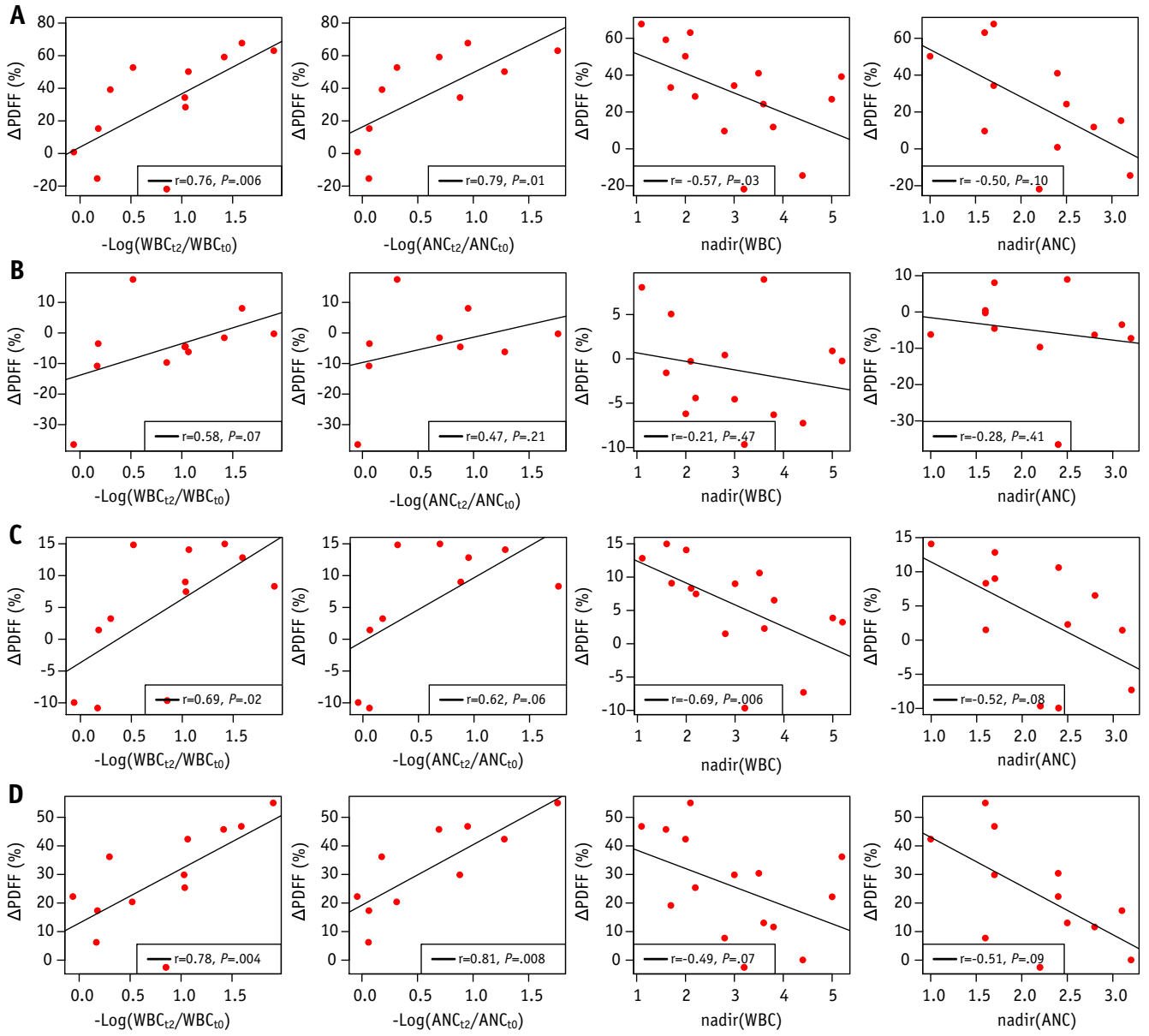

Fig. 3. Scatterplots and Spearman rank correlations for the difference in PDFF(%) versus peripheral blood cell counts by (A) C3-S2, (B) C3-T9, (C) T10-L3, and (D) L4-S2. PDFF = proton density fat fraction.

did not observe significant differences between treatment groups for the C3-T9 or T10-L3 region. Of note, when we did not control for region, we also observed a significant difference in the change in PDFF(%) per visit within C3-S2 (4.58% per visit, 95% CI: 0.52%-8.64%, $P = .03$).

Figure 3 shows scatterplots and Spearman rank correlations for ΔPDFF(%) versus peripheral blood cell counts for C3-S2 (Fig. 3A) and by each vertebral region (Fig. 3 B-D). Significant positive correlations were observed between ΔPDFF(%) and $-\log(WBC_{t2}/WBC_{t0})$ for T10-L3 ($r = 0.69$, $P = .02$), L4-S2 ($r = 0.78$, $P = .004$), and C3-S2 ($r = 0.76$, $P = .006$), indicating that increasing fat fraction correlates with decreasing WBC counts over the course of treatment. Similarly, significant correlations were observed between ΔPDFF(%) and $-\log(ANC_{t2}/ANC_{t0})$ for L4-S2 ($r = 0.81$, $P = .008$) and C3-S2 ($r = 0.79$, $P = .01$) and was borderline for T10-L3 ($r = 0.62$, $P = .06$). No significant correlations between ΔPDFF(%) and $-\log(WBC_{t2}/WBC_{t0})$ or $-\log(ANC_{t2}/ANC_{t0})$ were observed within C3-T9.

We also observed significant negative correlations between ΔPDFF(%) and WBC nadirs within C3-S2 ($r = -0.57$, $P = .03$) and T10-L3 ($r = -0.69$, $P = .006$), and a borderline significant correlation for L4-S2 ($r = -0.49$, $P = .07$), indicating an association between increased fat fraction and lower blood count nadirs. Similarly, we observed borderline significant negative correlations between ΔPDFF(%) and ANC nadirs within C3-S2 ($r = -0.50$, $P = .10$), T10-L3 ($r = -0.52$, $P = .08$), and L4-S2 ($r = -0.51$, $P = .09$). No significant correlations

between ΔPDFF(%) and WBC and ANC nadirs were observed within C3-T9.

Discussion

Multiple studies indicate that increased radiation dose to pelvic bone marrow is associated with greater hematologic toxicity in patients undergoing chemoradiation therapy (11, 17-25). Modern RT techniques can allow the incorporation of functional bone marrow imaging to specifically avoid hematopoietically active marrow subregions, which may reduce hematologic toxicity and increase chemotherapy tolerance (18, 24, 26).

In this study, we used IDEAL-IQ to compare changes in vertebral bone marrow fat fraction in patients undergoing highly myelotoxic chemoradiation therapy versus less myelotoxic chemoradiation therapy or RT alone. Overall, we observed that cumulative mean dose leads to significant increases in PDFF(%) within the vertebral bone marrow. These changes in PDFF(%) also corresponded to decreasing peripheral blood cell counts. In the highly myelotoxic group, we observed significant increases in PDFF(%) over the course of treatment within (eg, L4-S2) and above the pelvic radiation field (eg, T10-L3), even in patients who did not undergo extended field RT. Increases in PDFF(%) within the pelvic radiation field were significantly more pronounced in the highly myelotoxic group relative to that in the less myelotoxic group. Altogether these findings suggest that IDEAL is sensitive to marrow composition changes resulting from chemotherapy and radiation and that locoregional radiation effects contribute to the manifestation of clinical myelosuppression, particularly in patients undergoing myelotoxic chemotherapy.

Although conventional MR imaging may broadly distinguish red from yellow bone marrow (27), quantifying subtle gradations within red marrow in response to radiation therapy is possible only by using recent advances in MR fat quantification methodology (6, 12, 28-31). The use of MR with fat quantification allows noninvasive monitoring of the spatial effects of RT and to quantify the degree of red marrow damage as a function of radiation dose. This allows us to model and estimate the impact of conformal radiation techniques on red bone marrow injury.

This study had several limitations. There is significant heterogeneity in the population. To a degree, this heterogeneity was useful to estimate the impact of varying conditions on changes in marrow fat composition; however, further studies are ongoing in more homogeneous populations to control effects of treatment and demographic factors that could influence our findings (32). This longitudinal study included a relatively small sample and was subject to dropout, reducing our statistical power. Although we do not suspect this would have biased our primary effect estimates, this may have limited our ability to detect significant differences in the effects of chemotherapy in regions superior to the pelvic field. Our model form does assume a linear rate of change in fat fraction according to treatment group and spatial location, which may or may not be valid. However, the linear time model has the advantage of simplicity and parsimony and appeared to model the data well.

Conclusions

In summary, we observed increases in bone marrow fat composition over the course of treatment occurring specifically within the radiation treatment field, particularly in the presence of concurrent myelotoxic chemotherapy. These findings indicate that locoregional effects of RT likely significantly contribute to the clinical manifestation of myelosuppression in this setting. Modern RT techniques specifically designed to spare functioning bone marrow may reduce myelosuppression and permit better tolerance to myelotoxic chemotherapy regimens.

References

1. Sacks EL, Goris ML, Glatstein E, et al. Bone marrow regeneration following large field radiation: Influence of volume, age, dose, and time. *Cancer* 1978;42:1057-1065.
2. Georgiou KR, Foster BK, Xian CJ. Damage and recovery of the bone marrow microenvironment induced by cancer chemotherapy—potential regulatory role of chemokine CXCL12/receptor CXCR4 signaling. *Curr Mol Med* 2010;10:440-453.
3. Blankenberg FG. In vivo detection of apoptosis. *J Nucl Med* 2008;49:81S.
4. Crawford J, Dale DC, Lyman GH. Chemotherapy-induced neutropenia: risks, consequences, and new directions for its management. *Cancer* 2004;100:228-237.
5. Elting LS, Rubenstein EB, Martin CG, et al. Incidence, cost, and outcomes of bleeding and chemotherapy dose modification among solid tumor patients with chemotherapy-induced thrombocytopenia. *J Clin Oncol* 2001;19:1137-1146.
6. Reeder SB, Pineda AR, Wen Z, et al. Iterative decomposition of water and fat with echo asymmetry and least-squares estimation (IDEAL): Application with fast spin-echo imaging. *Magn Reson Med* 2005;54:636-644.
7. Rosen BR, Fleming DM, Kushner DC, et al. Hematologic bone marrow disorders: Quantitative chemical shift MR imaging. *Radiology* 1988;169:799-804.
8. Johnson LA, Hoppel BE, Gerard EL, et al. Quantitative chemical shift imaging of vertebral bone marrow in patients with Gaucher disease. *Radiology* 1992;182:451-455.
9. Brix G, Heiland S, Bellemann ME, et al. MR imaging of fat-containing tissues: Valuation of two quantitative imaging techniques in comparison with localized proton spectroscopy. *Magn Reson Imaging* 1993;11:977-991.
10. Liney GP, Bernard CP, Manton DJ, et al. Age, gender, and skeletal variation in bone marrow composition: A preliminary study at 3.0 Tesla. *J Magn Reson Imaging* 2007;26:787-793.
11. Liang Y, Bydder M, Yashar CM, et al. Prospective study of functional bone marrow-sparing intensity modulated radiation therapy with concurrent chemotherapy for pelvic malignancies. *Int J Radiat Oncol Biol Phys* 2013;85:406-414.
12. Bolan PJ, Arentsen L, Sueblinvong T, et al. Water-Fat MRI for assessing changes in bone marrow composition due to radiation and

chemotherapy in gynecologic cancer patients. *J Magn Reson Imaging* 2013;38:1578-1584.
13. Rosset A, Spadola L, Ratib O. OsiriX: An open-source software for navigating in multidimensional DICOM images. *J Digit Imaging* 2004;17:205-216.
14. Pinheiro J, Bates D, DebRoy S, et al. Linear and Nonlinear Mixed Effects Models. R package version 3.1-117. http://CRAN.R-project.org/package=nlme. Accessed November 13, 2013.
15. Laird NM, Ware JH. Random-effects models for longitudinal data. *Biometrics* 1982;38:963-974.
16. Gilmour AR, Thompson R, Cullis BR. Average information REML: An efficient algorithm for variance parameter estimation in linear mixed models. *Biometrics* 1995;51:1440-1450.
17. Mell LK, Kochanski JD, Roeske JC, et al. Dosimetric predictors of acute hematologic toxicity in cervical cancer patients treated with concurrent cisplatin and intensity-modulated pelvic radiotherapy. *Int J Radiat Oncol Biol Phys* 2006;66:1356-1365.
18. Mell LK, Schomas DA, Salama JK, et al. Association between bone marrow dosimetric parameters and acute hematologic toxicity in anal cancer patients treated with concurrent chemotherapy and intensity-modulated radiotherapy. *Int J Radiat Oncol Biol Phys* 2008;70:1431-1437.
19. Rose BS, Aydogan B, Liang Y, et al. Normal tissue complication probability modeling of acute hematologic toxicity in cervical cancer patients treated with chemoradiotherapy. *Int J Radiat Oncol Biol Phys* 2011;79:800-807.
20. Rose BS, Liang Y, Lau SK, et al. Correlation between radiation dose to ^{18}F-FDG-PET defined active bone marrow subregions and acute hematologic toxicity in cervical cancer patients treated with chemoradiotherapy. *Int J Radiat Oncol Biol Phys* 2012;83:1185-1191.
21. Liang Y, Messer K, Rose BS, et al. Impact of bone marrow radiation dose on acute hematologic toxicity in cervical cancer: Principal component analysis on high dimensional data. *Int J Radiat Oncol Biol Phys* 2010;78:912-919.
22. Klopp AH, Moughan J, Portelance L, et al. Hematologic toxicity in RTOG 0418: A phase 2 study of postoperative IMRT for gynecologic cancer. *Int J Radiat Oncol Biol Phys* 2013;86:83-90.
23. Bazan JG, Luxton G, Mok EC, et al. Normal tissue complication probability modeling of acute hematologic toxicity in patients treated with intensity-modulated radiation therapy for squamous cell carcinoma of the anal canal. *Int J Radiat Oncol Biol Phys* 2012;84:700-706.
24. McGuire SM, Menda Y, Ponto LL, et al. A methodology for incorporating functional bone marrow sparing in IMRT planning for pelvic radiation therapy. *Radiother Oncol* 2011;99:49-54.
25. Bazan JG, Luxton G, Kozak MM, et al. Impact of chemotherapy on normal tissue complication probability models of acute hematologic toxicity in patients receiving pelvic intensity modulated radiation therapy. *Int J Radiat Oncol Biol Phys* 2013;87:983-991.
26. Liang Y, Kim GY, Pawlicki T, et al. Feasibility study on dosimetry verification of volumetric-modulated arc therapy-based total marrow irradiation. *J Appl Clin Med Phys* 2013;14:3852.
27. Blomlie V, Rofstad EK, Skjønsberg A, et al. Female pelvic bone marrow: Serial MR imaging before, during, and after radiation therapy. *Radiology* 1995;194:537-543.
28. Liu CY, McKenzie CA, Yu H, et al. Fat quantification with IDEAL gradient echo imaging: Correction of bias from T(1) and noise. *Magn Reson Med* 2007;58:354-364.
29. Bydder M, Yokoo T, Hamilton G, et al. Relaxation effects in the quantification of fat using gradient echo imaging. *Magn Reson Imaging* 2008;26:347-359.
30. Yu H, McKenzie CA, Shimakawa A, et al. Multiecho reconstruction for simultaneous water-fat decomposition and T2* estimation. *J Magn Reson Imaging* 2007;26:1153-1161.
31. Chebrolu VV, Hines CDG, Yu H, et al. Independent estimation of T-2 for water and fat for improved accuracy of fat quantification. *Magn Reson Med* 2010;63:849-857.
32. Mell LK. Intensity modulated radiation therapy for gynecologic malignancies: A testable hypothesis. *Int J Radiat Oncol Biol Phys* 2012;84:566-568.